Endothelial Chromosome 13 Deletion in Congenital Heart Disease–associated Pulmonary Arterial Hypertension Dysregulates *SMAD9* Signaling

To the Editor:

Pulmonary arterial hypertension (PAH) is a complex and progressive disorder characterized by the development of vascular lesions and aberrant vascular remodeling that results in elevated pulmonary vascular resistance and right-heart failure (1, 2). The predominant histopathologic findings are muscularization of the arteries and arterioles and the presence of plexiform lesions composed of proliferative endothelial cells and myofibroblasts (1, 3). PAH can be idiopathic, heritable, or associated with conditions such as congenital heart defects (4). Congenital heart disease–associated PAH (APAH-CHD) most commonly occurs with systemic-to-pulmonary shunt lesions (5) and accounts for approximately 10% of all patients with PAH (6). The shunt increases pressure in the pulmonary arteries, leading to abnormal shear stress, circumferential wall stretch, endothelial dysfunction, and ultimately PAH (5). Although the phenotype of the APAH-CHD right ventricle differs from idiopathic PAH and heritable PAH (HPAH), the changes at the level of the lung microvasculature and the endothelium are very similar (5). We have recently shown that endothelial cells isolated from the explant lungs of patients with PAH frequently harbor somatic chromosome abnormalities (7). Here we describe functional analysis of a heterozygous large interstitial deletion of chromosome 13 (del-13) in pulmonary artery endothelial cells (PAEC) from a patient with APAH-CHD. Some of the results of these studies have been previously reported in the form of abstracts (8, 9).

The patient was diagnosed with atrial and ventricular septal defects in her teens but was not closed until age 42 years, at which time pulmonary hypertension was present. She initially did well after surgery, but her PAH ultimately worsened to New York Heart Association class IV, and she required lung transplantation. Additional clinical information is included in the online supplement. Histologic examination of the explant lung tissue revealed a classic idiopathic PAH-type pathology with plexiform lesions, media hypertrophy, and intima remodeling (Figures 1A–1C). As detailed in the online supplement, genome-wide single-nucleotide polymorphism array analysis identified an interstitial deletion of chromosome 13 in approximately 70% of PAEC in culture (Figure 1D). Whole lung tissue and cultured pulmonary artery smooth muscle cells (PASMC) from the same individual showed no detectable abnormalities, confirming that this is a lineage-specific somatic change. X-inactivation analysis confirmed a near-clonal PAEC population, whereas PASMC were polyclonal (Figure 1F).

The deletion interval is 77 Mb in size and spans the region from 13q12.2 to 13q33.3 (Figure 1E). To further characterize the deletion, we performed polymerase chain reaction amplification across the proximal and distal breakpoints. Sanger sequencing revealed a clean fusion of the chromosome between position Chr13:27,927,328 and Chr13:104,891,919 (human genome build 19) (Figure 1E). Both the distal and proximal sites of the deletion show a paucity of microsatellite repeats, copy number variations, or CpG islands that might have predisposed to double-strand breaks. Thus the del-13 breakpoints appear random and could be a result of reactive oxygen species or topoisomerase failures. *SMAD9* (protein: SMAD8), a gene mutated in a small number of HPAH cases (10–12), is the only protein-coding gene in the deleted interval known to play a role in PAH. Table E1 in the online supplement lists additional genes that are within the deleted region and expressed in PAEC, including the tumor suppressor gene *RB1*. Table E2 in the online supplement lists the small RNA species within the deleted interval, which includes the miR-17∼92 microRNA cluster. Inhibition of miR-17 has been shown to improve lung function in experimental pulmonary hypertension; thus, its deletion would seem unlikely to contribute to the pathogenesis of PAH in this patient (13).

To confirm that the deletion was present *in vivo* at the time of lung explant, fluorescence *in situ* hybridization analysis was performed on formalin-fixed, paraffin-embedded tissue sections (Figures 1G–1J). Tissue from a rejected donor lung was used as control. A probe for the *RB1* gene (13q14) was used in conjunction with a 13q34 probe that binds outside the deleted interval. Fluorescence *in situ* hybridization signals in the endothelial cells lining the vessel walls were counted, and comparisons were made between patient and control cells, as well as to adjacent smooth muscle cells of the same vessels and normal airway epithelium on the same slide. Slides from three different lung lobes were analyzed: lower right, middle right, and lower left. To avoid artifacts caused by nuclear truncation, only cells with two 13q34 signals were scored. Cells were analyzed from pulmonary arterioles approximately 50–100 μm in diameter. The endothelial lineage of cells was defined by CD31-positive staining of serial sections. In control lung sections, there was no significant difference in the distribution of *RB1* signals between endothelial, smooth muscle, and airway epithelial cells ($\chi^2 = 4.96$; $P = 0.291$), whereas in the patient lung, there was a significant difference between the cell types ($\chi^2 = 53.84$; $P < 0.001$). Endothelial cells in the patient lung exhibited a highly significant difference in the *RB1* hybridization pattern compared with control endothelial cells ($\chi^2 = 59.64$; $P < 0.001$). A one-tailed z-ratio test confirmed a significant increase in the number of cells with a single *RB1* signal compared with control ($P < 0.001$), consistent with the deletion seen on the array. Results were significant across each of the three lung lobes studied (Table 1). In contrast, airway epithelium showed no significant difference in hybridization pattern compared with the control donor lung. Collectively, smooth muscle cells also showed no significant difference between patient and control ($\chi^2 = 5.72$; $P = 0.057$; z-ratio $P = 0.08$). When the results from individual lobes were analyzed separately, the distribution of signals was significantly different in the middle right lobe ($\chi^2 = 8.59$; $P = 0.014$),

Supported in part by the National Heart, Lung and Blood Institute of the National Institutes of Health under award numbers R01HL098199, R03HL110831, and RC37HL60917.

Author Contributions: K.M.D. and M.A.A. designed the study; acquired, analyzed, and interpreted data; and wrote the manuscript. S.A.C. and S.C.E. acquired samples, established cells, and reviewed the clinical information. R.M.T. reviewed and interpreted the pathology. All authors contributed to writing the manuscript.

This letter has an online supplement, which is accessible from this issue's table of contents at www.atsjournals.org

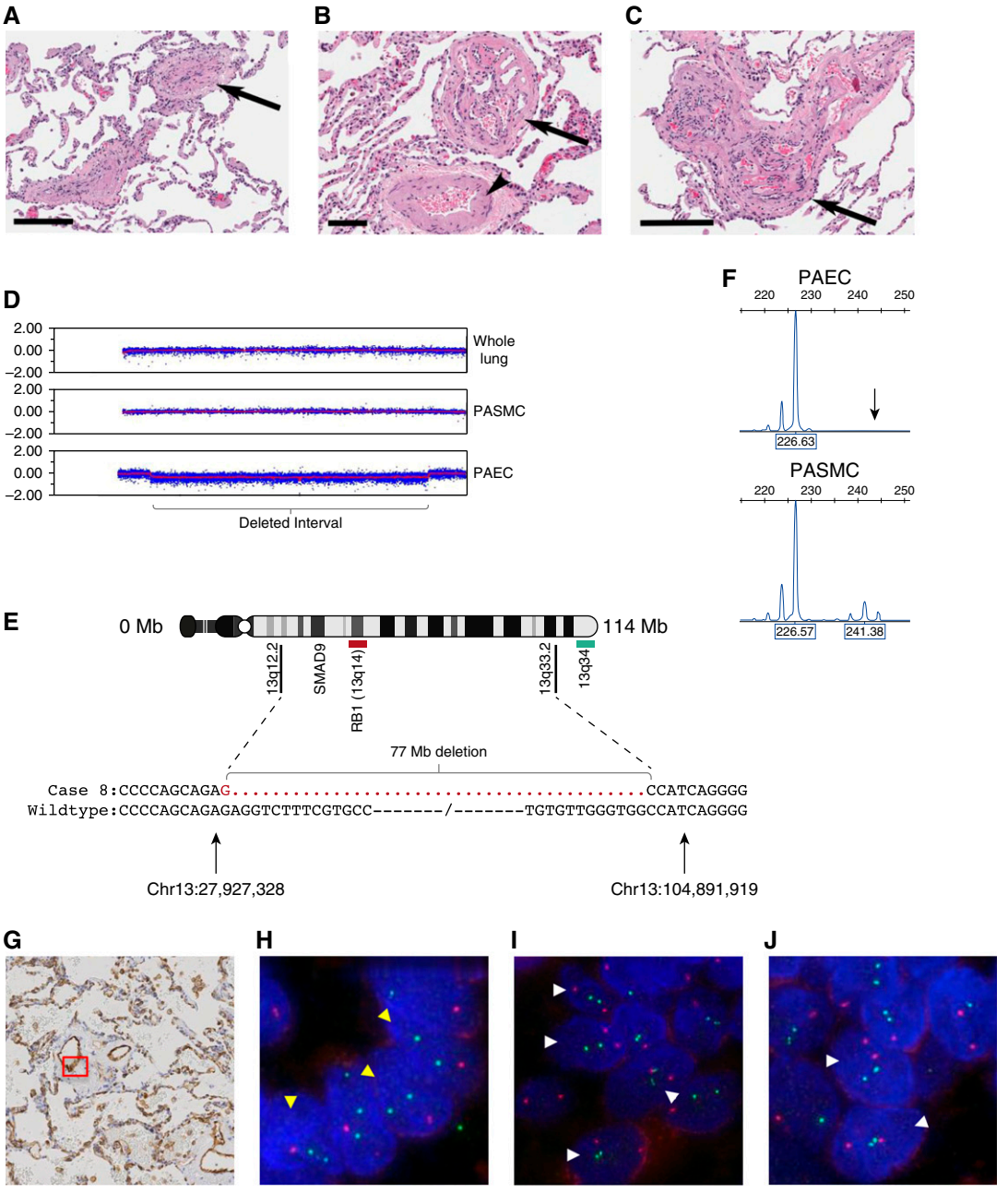

Figure 1. Pulmonary artery endothelial cells (PAEC) from a patient with congenital heart disease–associated pulmonary arterial hypertension exhibit a large interstitial deletion of chromosome 13. (*A*–*C*) Hematoxylin and eosin–stained sections of the lung. (*A*) Intima obliteration of muscular pulmonary artery (*arrow*). Note reduced vascular lumen with prominent media and intima. (*B*) Plexiform lesion with multiple channels lined by endothelial-like cells (*arrows*) and collagen-rich intraluminal septa. The parent pulmonary artery shows media hypertrophy (*arrowhead*). (*C*) Fully developed plexiform lesion with clusters of endothelial-like cells. (*D*) Single-nucleotide polymorphism array analysis of whole lung tissue and cultured pulmonary artery smooth muscle cells (PASMC) demonstrated a normal profile, with the log-R ratio, a measure of signal intensity on the array, clustered around 0.0. In primary PAEC, the log-R deviates below 0.0, indicating an interstitial deletion at 13q12.2–q33.2 (*bracket*). (*E*) Ideogram of chromosome 13 showing region of loss, enlarged to show the deletion is 77 Mb in size and spans Chr13: 27,927,328–104,891,919. The positions of the *RB1* (*red*) and 13q34 (*green*) probes used for fluorescence *in situ* hybridization are shown. (*F*) Amplification of cDNA at the androgen receptor locus on the X chromosome demonstrates a biallelic expression pattern with alleles of 226 and 241 bp in PASMC. In PAEC, the 241-bp allele (*arrow*) is absent, indicating that X-inactivation is nonrandom and the del-13 PAEC are clonal. (*G*) CD-31–stained section of explant patient lung tissue; *red box* indicates the location of endothelial cells shown in *H*. (*H*) Fluorescence *in situ* hybridization image of patient endothelial cell nuclei hybridized with the *RB1* probe (*red*) and 13q34 (*green*). Nuclei exhibiting the interstitial chromosome 13 deletion are indicated with *yellow arrowheads*. (*I*) Fluorescence *in situ* hybridization showing adjacent patient smooth muscle cell nuclei. Nuclei with two *RB1* and 13q34 probes are indicated with *white arrowheads*. (*J*) Fluorescence *in situ* hybridization of control explant lung tissue from a failed donor lung. Normal nuclei are indicated with *white arrowheads*. Nuclei with only one 13q34 signal were not scored. *Scale bars*: *A* and *C*, 200 μm; *B*, 90 μm.

but not in the other two lobes (Table 1). However, the z-ratio indicated there was no significant difference in the proportion of cells monosomic for *RB1* ($P = 0.13$). The aberrant signal pattern was mainly confined to three adjacent vessels on this slide and may represent either a technical artifact or a highly localized abnormality. Together, these results suggest a widespread deletion of chromosome 13 in endothelial cells across at least three lobes of the right and left lung, whereas smooth muscle cells appear largely normal and any abnormality is confined to a small number of vessels.

SMAD9 is part of the bone morphogenetic protein (BMP) signaling cascade, downstream of the type 2 BMP receptor, *BMPR2*, the gene mutated in the majority of HPAH cases. We have previously shown that PAEC and PASMC from a patient with a heterozygous germline *SMAD9*:R294X mutation exhibit a hyperproliferative phenotype, blunted BMP signaling, and dysregulated Smad-mediated microRNA processing (10). Overexpression of wild-type *SMAD9* can correct these defects (10). Given that *SMAD9* is the only gene within the del-13 deletion previously associated with PAH, we hypothesized that the proliferation, BMP responsiveness, and Smad-mediated microRNA processing in del-13 PAEC would be similar to *SMAD9*:R294X cells.

Real-time polymerase chain reaction analysis of del-13 PAEC confirmed a decreased level of *SMAD9* expression, similar to that of R294X (Figure E1). Del-13 PAEC indeed proliferated faster than controls at baseline and were comparable to *SMAD9*:R294X PAEC (Figure E2A; $P < 0.001$). In contrast, proliferation of the cytogenetically normal PASMC was similar to that of control cells (Figure E2B). Analysis of miR processing in del-13 and R294X cells was undertaken, and both showed a failure to up-regulate *miR-27a* levels after BMP9 treatment compared with controls (Figure E2C). In contrast, chromosomally normal PASMC were indistinguishable from control cells (Figure E2D). Similar results were obtained for *miR-21* and *miR-100* (data not shown). *ID1* induction, a marker of canonical BMP signaling, was reduced in del-13 PAEC, but not PASMC, after BMP treatment (Figure E2D). Western blot analysis of del-13 PAEC revealed diminished Smad-1/5/8 phosphorylation (Figure E3A) and blunted ID1 up-regulation when compared with control cells (Figure E3B). These results are again consistent with the R294X cells. BMPR-II expression was normal (Figure E3C). Detailed methods are contained in the online supplement. Overexpression of *SMAD9* in del-13 PAEC by introduction of a cDNA expression construct normalized their baseline proliferation rate (Figure E4A) and restored the additional growth suppressive effects of BMP9 stimulation (Figure E4B). miR processing and canonical BMP signaling were also normalized (Figures E3C and E3D). Together, these results suggest that despite the large number of chromosome 13 genes deleted in these cells, their hyperproliferation, dysregulated miR processing, and

Table 1. Results of Fluorescence *In Situ* Hybridization Analysis

Lobe of the Lung and Cells Studied	*RB1* Signals per Nucleus			Total Nuclei	Chi-Square Contingency Analysis	Increase in Proportion of Cells Monosomic for *RB1* (One-tailed z Ratio)
	2	1	0			
Lower right lobe						
Endothelial cells					$P = 0.007$	14.0%, $P = 0.010$
Patient	42	31	27	100		
Control	64	17	19	100		
Airway epithelium					ns	ns
Patient	32	6	12	50		
Control	33	10	7	50		
Smooth muscle cells					ns	ns
Patient	66	21	13	100		
Control	69	16	15	100		
Middle right lobe						
Endothelial cells					$P < 0.001$	16.0%, $P < 0.001$
Patient	78	70	52	200		
Control	123	38	39	200		
Airway epithelium					ns	ns
Patient	60	15	25	100		
Control	66	16	18	100		
Smooth muscle cells					$P = 0.014$	ns
Patient	83	36	31	150		
Control	106	28	16	150		
Lower left lobe						
Endothelial cells					$P < 0.001$	17.0%, $P = 0.002$
Patient	38	32	30	100		
Control	68	15	17	100		
Airway epithelium					ns	ns
Patient	35	5	10	50		
Control	35	8	7	50		
Smooth muscle cells					ns	ns
Patient	63	21	16	100		
Control	67	19	14	100		

Definition of abbreviations: ns = not significant.

BMP response is largely accounted for by the heterozygous deletion of *SMAD9*.

Lung development begins as a simple outpouching of the foregut and develops by branching morphogenesis into a highly complex organ (14). Interestingly, a recent study showed that in mice, the pulmonary vasculature develops even in the absence of lung development and is derived from a population of multipotent cardiopulmonary progenitor cells (15). Because of the timing and spacing of pulmonary branches within the lung, the presence of the chromosome 13 deletion in endothelial cells across three different lobes of the lung implies it may have been present early in lung vasculogenesis. An alternative explanation could be that the deletion occurred *in situ* during endothelial injury resulting from shear stress. However, because it is unlikely that the same deletion would have arisen multiple times in different parts of the lung, this model would have required active division of a single mutant cell and widespread dispersal in the mature lung. It is also notable that the vessels scored in this study are primarily large precapillary vessels that are not subject to the same hemodynamically induced alterations in endothelial function as the microvasculature. Ultimately, however, there is no way to distinguish between these two hypotheses, and shear stress likely contributes to disease progression in multiple other ways, promoting endothelial dysfunction and increasing apoptosis resistance (16).

The deletion identified in the lung of this patient is clearly a postzygotic event, as wild-type cells are also present. The functional differences in BMP signaling between del-13 and wild-type cells suggest the deletion may have contributed to PAH pathogenesis. Other precedents for somatic mosaicism contributing to the pathogenesis of vascular disorders include the presence of acquired mutations in the endothelial cells of cerebral cavernous malformations (17). Furthermore, somatic mutations in the BMP genes *ACVRL1* and *ENG* have been reported in hereditary hemorrhagic telangiectasia (18–21). Hereditary hemorrhagic telangiectasia is an endothelial vascular condition, and the disease can manifest when $\leqslant$20% of cells carry the mutation (18). Notably, two of the seven hereditary hemorrhagic telangiectasia cases reported with postzygotic mutations also had PAH (19, 20).

BMP signaling plays a critical role in cardiac development, and mouse knockout studies have shown that BMP signaling is crucial in the regulation of septovalvular development (22). Studies undertaken to determine the prevalence of PAH-associated mutations in the APAH-CHD population indicate that up to 10% have a germline *BMPR2* mutation (23). Given that the *Smad9* knockout mouse has defective vascular remodeling (24), it is therefore tempting to speculate that the del-13 abnormality might also be present in the heart of this patient, perhaps even contributing to the primary CHD. However, no other tissues were available for analysis.

In conclusion, deletion of chromosome 13q12.2-q33.2 in PAEC from a patient with APAH-CHD confers significant changes in BMP signaling, rendering them indistinguishable from HPAH cells with a germline *SMAD9* mutation. In contrast, cultured PASMC from the same patient are karyotypically normal and show normal BMP signaling. Although the exact timing of this chromosome rearrangement cannot be determined, its widespread distribution within the lung suggests it may have been present during lung vasculogenesis. On a background of genetic susceptibility (del-13), we hypothesize that PAH would arise in this patient as a result of an initiating stimulus or injury, such as hypoxia, shear stress, or inflammation. This case therefore provides the first evidence that somatic chromosome abnormalities in the PAH lung can confer functionally relevant changes and suggests they may constitute a predisposing event that contributes to vascular remodeling. ■

Author disclosures are available with the text of this letter at www.atsjournals.org.

Acknowledgment: The authors thank the patients who consented to use of their tissues in this study, Lori Mavrakis and the Cleveland Clinic Pathobiology Tissue and Cell Culture Core for cells, Munir Tanas and the Lerner Research Institute Imaging Core for help with fluorescence *in situ* hybridization and imaging, and the Lerner Research Institute Genomics Core for microarray and sequencing services.

Kylie M. Drake, Ph.D.
Suzy A. Comhair, Ph.D.
Serpil C. Erzurum, M.D.
Cleveland Clinic
Cleveland, Ohio

Rubin M. Tuder, M.D.
University of Colorado
Aurora, Colorado

Micheala A. Aldred, Ph.D.
Cleveland Clinic
Cleveland, Ohio

References

1. Humbert M, Morrell NW, Archer SL, Stenmark KR, MacLean MR, Lang IM, Christman BW, Weir EK, Eickelberg O, Voelkel NF, *et al*. Cellular and molecular pathobiology of pulmonary arterial hypertension. *J Am Coll Cardiol* 2004;43(12 Suppl S):13S–24S.
2. Rubin LJ. Primary pulmonary hypertension. *N Engl J Med* 1997;336: 111–117.
3. Tuder RM, Groves B, Badesch DB, Voelkel NF. Exuberant endothelial cell growth and elements of inflammation are present in plexiform lesions of pulmonary hypertension. *Am J Pathol* 1994;144:275–285.
4. Simonneau G, Robbins IM, Beghetti M, Channick RN, Delcroix M, Denton CP, Elliott CG, Gaine SP, Gladwin MT, Jing ZC, *et al*. Updated clinical classification of pulmonary hypertension. *J Am Coll Cardiol* 2009;54(1 Suppl):S43–S54.
5. Krishnan U, Rosenzweig EB. Pulmonary arterial hypertension associated with congenital heart disease. *Clin Chest Med* 2013;34:707–717.
6. Badesch DB, Raskob GE, Elliott CG, Krichman AM, Farber HW, Frost AE, Barst RJ, Benza RL, Liou TG, Turner M, *et al*. Pulmonary arterial hypertension: baseline characteristics from the REVEAL Registry. *Chest* 2010;137:376–387.
7. Aldred MA, Comhair SA, Varella-Garcia M, Asosingh K, Xu W, Noon GP, Thistlethwaite PA, Tuder RM, Erzurum SC, Geraci MW, *et al*. Somatic chromosome abnormalities in the lungs of patients with pulmonary arterial hypertension. *Am J Respir Crit Care Med* 2010;182:1153–1160.
8. Aldred MA, Federici C, Comhair SAA, Erzurum SC, Drake KM. Somatic deletion of *SMAD9* in congenital heart disease-associated pulmonary arterial hypertension leads to altered microRNA processing and cell hyperproliferation [abstract]. *Am J Respir Crit Care Med* 2012;185: A6514.
9. Drake KM, Aldred MA. Distribution of a functionally significant somatic deletion of chromosome 13 in the lung of associated pulmonary arterial hypertension suggests an early developmental origin [abstract]. *Am J Respir Crit Care Med* 2014;189:A6618.
10. Drake KM, Zygmunt D, Mavrakis L, Harbor P, Wang L, Comhair SA, Erzurum SC, Aldred MA. Altered MicroRNA processing in heritable pulmonary arterial hypertension: an important role for Smad-8. *Am J Respir Crit Care Med* 2011;184:1400–1408.
11. Nasim MT, Ogo T, Ahmed M, Randall R, Chowdhury HM, Snape KM, Bradshaw TY, Southgate L, Lee GJ, Jackson I, *et al*. Molecular

genetic characterization of SMAD signaling molecules in pulmonary arterial hypertension. *Hum Mutat* 2011;32:1385–1389.
12. Shintani M, Yagi H, Nakayama T, Saji T, Matsuoka R. A new nonsense mutation of *SMAD8* associated with pulmonary arterial hypertension. *J Med Genet* 2009;46:331–337.
13. Pullamsetti SS, Doebele C, Fischer A, Savai R, Kojonazarov B, Dahal BK, Ghofrani HA, Weissmann N, Grimminger F, Bonauer A, *et al*. Inhibition of microRNA-17 improves lung and heart function in experimental pulmonary hypertension. *Am J Respir Crit Care Med* 2012;185:409–419.
14. Metzger RJ, Klein OD, Martin GR, Krasnow MA. The branching programme of mouse lung development. *Nature* 2008;453:745–750.
15. Peng T, Tian Y, Boogerd CJ, Lu MM, Kadzik RS, Stewart KM, Evans SM, Morrisey EE. Coordination of heart and lung co-development by a multipotent cardiopulmonary progenitor. *Nature* 2013;500:589–592.
16. Dimmeler S, Haendeler J, Rippmann V, Nehls M, Zeiher AM. Shear stress inhibits apoptosis of human endothelial cells. *FEBS Lett* 1996; 399:71–74.
17. McDonald DA, Shi C, Shenkar R, Gallione CJ, Akers AL, Li S, De Castro N, Berg MJ, Corcoran DL, Awad IA, *et al*. Lesions from patients with sporadic cerebral cavernous malformations harbor somatic mutations in the CCM genes: evidence for a common biochemical pathway for CCM pathogenesis. *Hum Mol Genet* 2014;23:4357–4370.
18. Best DH, Vaughn C, McDonald J, Damjanovich K, Runo JR, Chibuk JM, Bayrak-Toydemir P. Mosaic *ACVRL1* and *ENG* mutations in hereditary haemorrhagic telangiectasia patients. *J Med Genet* 2011; 48:358–360.
19. Eyries M, Coulet F, Girerd B, Montani D, Humbert M, Lacombe P, Chinet T, Gouya L, Roume J, Axford MM, *et al*. *ACVRL1* germinal mosaic with two mutant alleles in hereditary hemorrhagic telangiectasia associated with pulmonary arterial hypertension. *Clin Genet* 2012;82:173–179.
20. McDonald J, Gedge F, Burdette A, Carlisle J, Bukjiok CJ, Fox M, Bayrak-Toydemir P. Multiple sequence variants in hereditary hemorrhagic telangiectasia cases: illustration of complexity in molecular diagnostic interpretation. *J Mol Diagn* 2009;11:569–575.
21. Lee NP, Matevski D, Dumitru D, Piovesan B, Rushlow D, Gallie BL. Identification of clinically relevant mosaicism in type I hereditary haemorrhagic telangiectasia. *J Med Genet* 2011;48:353–357.
22. van Wijk B, Moorman AF, van den Hoff MJ. Role of bone morphogenetic proteins in cardiac differentiation. *Cardiovasc Res* 2007;74:244–255.
23. Roberts KE, McElroy JJ, Wong WP, Yen E, Widlitz A, Barst RJ, Knowles JA, Morse JH. *BMPR2* mutations in pulmonary arterial hypertension with congenital heart disease. *Eur Respir J* 2004;24:371–374.
24. Huang Z, Wang D, Ihida-Stansbury K, Jones PL, Martin JF. Defective pulmonary vascular remodeling in Smad8 mutant mice. *Hum Mol Genet* 2009;18:2791–2801.

Genetic Heterogeneity of Circulating Cells from Patients with Lymphangioleiomyomatosis with and without Lung Transplantation

To the Editor:

Lymphangioleiomyomatosis (LAM) is a multisystem disease characterized by lung destruction, lymphatic abnormalities, and abdominal tumors (e.g., angiomyolipomas [AMLs]) (1). LAM may present sporadically or in association with tuberous sclerosis complex (TSC) and is found primarily with genetic alterations in the tumor suppressor gene *TSC2* (1). *TSC2* loss of heterozygosity (LOH) was first shown in AMLs and retroperitoneal lymph nodes isolated from patients with sporadic LAM (2). LAM cells are believed to be clonal, as the same pattern of *TSC2* LOH is seen in different organs (3, 4). LAM cells can metastasize (5, 6), and circulating LAM cells have been isolated from blood, urine, bronchoalveolar lavage fluid, and chylous effusions (7, 8). We reported 10 cases in which LAM cells from different body fluids showed differences in LOH patterns (8), suggesting that a patient may harbor different LAM cell clones. Here, we find that circulating LAM cells may exhibit extensive genetic heterogeneity.

Blood and urine samples were collected from 65 patients with LAM, 44 of whom have been studied previously (8, 9). The methods for fluorescence-activated cell sorting of circulating cells from blood and urine and for LOH determination are in the online supplement. LAM cells are defined genetically by *TSC2* LOH and phenotypically by reactivity to specific cell-surface markers. CD45 and CD235a help to identify LAM cells in blood (7, 8), whereas CD44v6 and CD9 are used with urine (8). The pattern of LOH of five microsatellite markers spanning the *TSC2* locus was noted.

On examination of *TSC2* LOH patterns seen in circulating cells from blood from 45 patients with LAM analyzed at one visit, 31 patients showed LOH in both blood subpopulations (Tables 1 and 2). Eight had a different pattern of LOH in the $CD45^-$, $CD235a^-$ population than in the $CD45^-$, $CD235a^+$ population (*see* Figure E1 in the online supplement; L80, L110, L363, L554, L47, L324, L697, L56). Age and TSC status did not affect the detection of genetic heterogeneity (Tables 1 and 2). Therefore, 25.8% of patients who showed LOH in both populations isolated from blood had evidence of circulating cells with different LOH patterns, suggesting that a single patient may have different clones of LAM cells.

LOH patterns were compared in urine and blood in 45 patients seen for one visit (Table 3). Ten patients (33.3% of patients who showed LOH in urine) showed differences in LOH

Table 1. Allelic Patterns Seen in Cells Isolated from Blood (Populations $CD45^-$, $CD235a^-$, and $CD45^-$, $CD235a^+$) of Patients with One Visit: Overall Distribution of *TSC2* Loss of Heterozygosity/Retention of Heterozygosity

TSC2 Status	No. (%) of Patients*	Mean Age ± SD (*yr*)	TSC (*n*)
ROH	4 (8.9)	50.1 ± 4.5	0
LOH in $CD45^-$, $CD235a^-$	2 (4.4)	45.3 ± 9.3	0
LOH in $CD45^-$, $CD235a^+$	8 (17.8)	52.1 ± 14.4	3
LOH in $CD45^-$, $CD235a^-$ and $CD45^-$, $CD235a^+$	31 (68.9)	47.5 ± 11.0	6

Definition of abbreviations: LOH = loss of heterozygosity; ROH = retention of heterozygosity; TSC = tuberous sclerosis complex.
TSC column shows the number of patients in that category who have tuberous sclerosis.
*N = 45 patients.

Supported by the Intramural Research Program of the National Institutes of Health, National Heart, Lung, and Blood Institute.

This letter has an online supplement, which is accessible from this issue's table of contents at www.atsjournals.org